Electronic Supplementary Material (ESI) for Dalton Transactions.
This journal is © The Royal Society of Chemistry 2017

Synthesis and Characterization of a Novel Aminopolycarboxylate Complexant for Efficient Trivalent *f*-element Differentiation: *N*-butyl-2-acetamide-diethylenetriamine-*N,N',N'',N''*-tetraacetic Acid

Colt R. Heathman[1*], Travis S. Grimes[1], Santa Jansone-Popova[2], Alexander S. Ivanov[2],
Vyacheslav S. Bryantsev[2], Peter R. Zalupski[1*]

General

The ^{1}H and ^{13}C NMR spectra were recorded on an AvanceIII-400 MHz NMR spectrometer (Bruker Company) equipped with a 5 mm PABBI probe. Residual solvent peak was used as an internal reference ($CDCl_3$: 7.26 ppm for ^{1}H NMR and 77.16 ppm for ^{13}C NMR; 1,4-dioxane in D_2O: 3.75 ppm for ^{1}H NMR and 67.19 ppm for ^{13}C NMR). HRMS analyses were performed under contract by UT Austin mass spectrometric facility using positive mode ESI method. Elemental analyses (EA) were performed under contract by Atlantic Microlab, Inc. of Norcross, GA. Commercially available compounds were purchased from Aldrich Chemical Co., Acros Organics, Alfa Aesar or TCI America and were used without further purification.

Synthesis Scheme

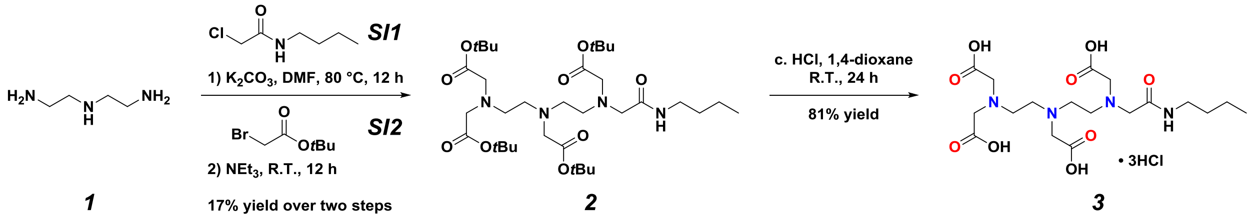

Synthesis

N-butyl-2-chloroacetamide (**SI1**) was prepared according to a literature procedure.[1]

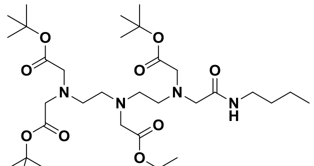

2

Compound **2**: To a mixture of diethylenetriamine **1** (5.0 mL, 46.1 mmol), K_2CO_3 (31.9 g, 0.23 mol) and DMF (154 mL) was added *N*-butyl-2-chloroacetamide (**SI1**, 6.9 g, 46.1 mmol). The reaction mixture was heated to 80 ^{0}C and stirred at this temperature for 12 h. Afterwards, this mixture was cooled down to room temperature and NEt_3 (51 mL, 0.37 mol) followed by tert-butyl 2-bromoacetate (**SI2**, 41 mL, 0.28 mol) were added *(slightly exothermic reaction!)*. The reaction mixture was allowed to stir at room temperature for 12 h. DI water was then added to this mixture and product extracted with diethyl ether (3x), organic phases were combined, washed with DI water, then brine and dried over anhydrous $MgSO_4$. After filtration, solvent was evaporated under reduced pressure on a rotary evaporator. The crude material was purified on CombiFlash R*f* automated flash chromatography system using normal phase silica gel as a stationary phase and gradient 20%-80% EtOAc in hexanes as an eluent system. The product was obtained as a light yellow, viscous oil (5.4 g, 17% yield). **^{1}H NMR** (400 MHz, $CDCl_3$) 7.93 (t, *J* = 5.6 Hz, 1H), 3.43 (s, 4H), 3.33-3.20 (m, 8H), 2.83-2.68 (m, 8H), 1.44 (s, 36H), 1.54-1.39 (m, 2H), 1.39-1.28 (m, 2H), 0.91 (t, *J* = 7.1 Hz, 3H). **^{13}C NMR** (100.66 MHz, $CDCl_3$) 171.5, 170.8, 170.7, 81.5, 81.1, 59.0, 57.1, 56.2, 56.0, 53.5, 52.8, 52.6, 52.1, 39.0, 28.31, 28.28, 20.3, 14.0. **HRMS** *m/z*: $[M+H]^+$, calculated for $C_{34}H_{64}N_4O_9$, 673.47460; found 673.47580.

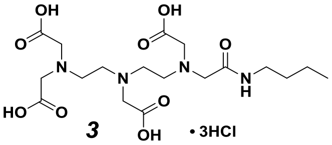

3

Compound (**3**). The solution of compound **2** (5.3 g, 7.9 mmol) in 24 mL of dry 1,4-dioxane was cooled in ice/water bath, to this solution concentrated hydrochloric acid (24 mL) was added slowly *(slightly exothermic reaction!)*. After 10 minutes, the reaction mixture was allowed to warm-up to room temperature and stir for 24 hours. The white precipitate formed was filtered, washed with diethyl ether and dried under vacuum at 50 ^{0}C for 12 h. The product was obtained as white, hygroscopic solid (3.56 g, 81% yield). **^{1}H NMR** (400 MHz, D_2O) 4.83 (s), 4.17 (s, 4H), 4.10 (d, *J* = 4.9 Hz, 4H), 3.75 (s, 1,4-dioxane), 3.71 (s, 2H), 3.56 (t, *J* = 6.3 Hz, 2H), 3.51 (t, *J* = 6.3 Hz, 2H), 3.30-3.17 (m, 6H), 1.56-1.44 (m, 2H), 1.38-1.25 (m, 2H), 0.88 (t, *J* = 7.4 Hz, 3H). **^{13}C NMR** (100.66 MHz, D_2O) 174.0, 169.9, 169.7, 166.2, 67.2 (CH_2, 1,4-dioxane), 56.9, 56.0, 54.4, 53.7, 50.3, 40.1, 30.9, 20.0, 13.5. **HRMS** *m/z*: $[M+H]^+$, calculated for $C_{18}H_{32}N_4O_9$, 449.22420; found 449.22490. **EA** calculated for $C_{18}H_{32}N_4O_9•(HCl)_3$: C, 38.76; H, 6.32; N, 10.04; Cl, 19.06; found: C, 38.15; H, 6.24; N, 9.83; Cl, 18.58.

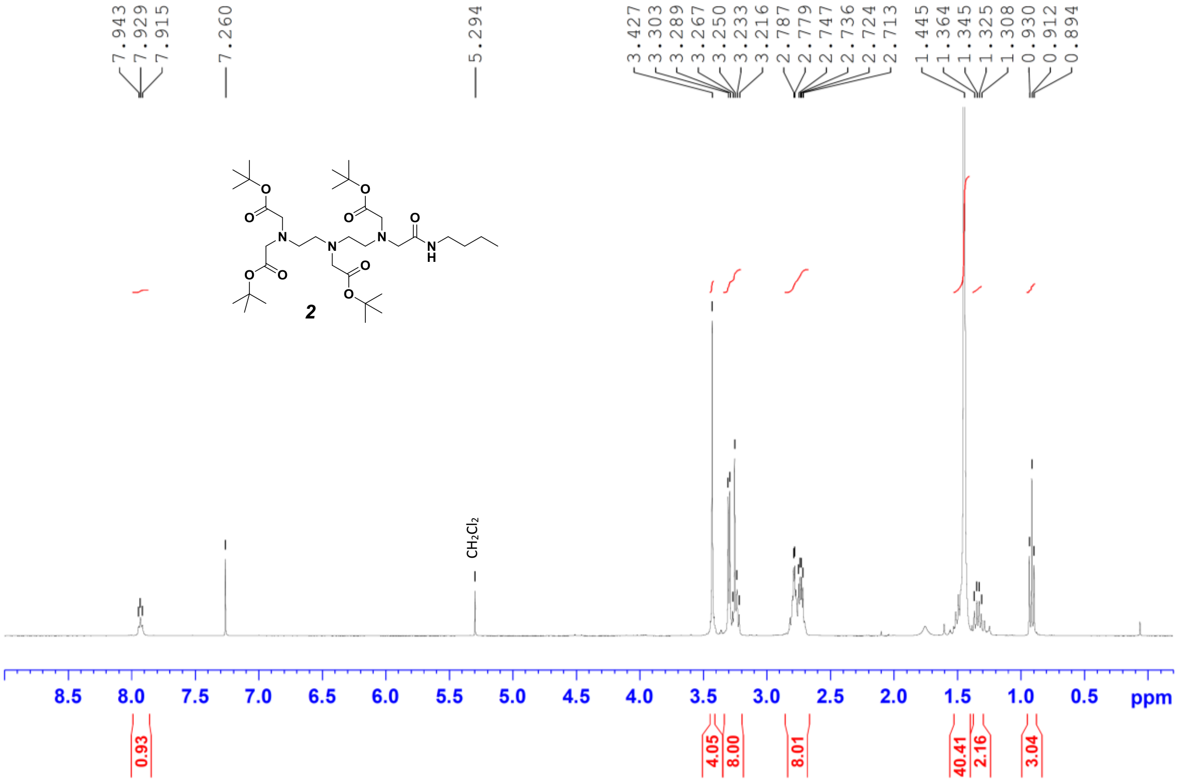

Figure SI-1. ^{1}H NMR spectrum of **2** in $CDCl_3$.

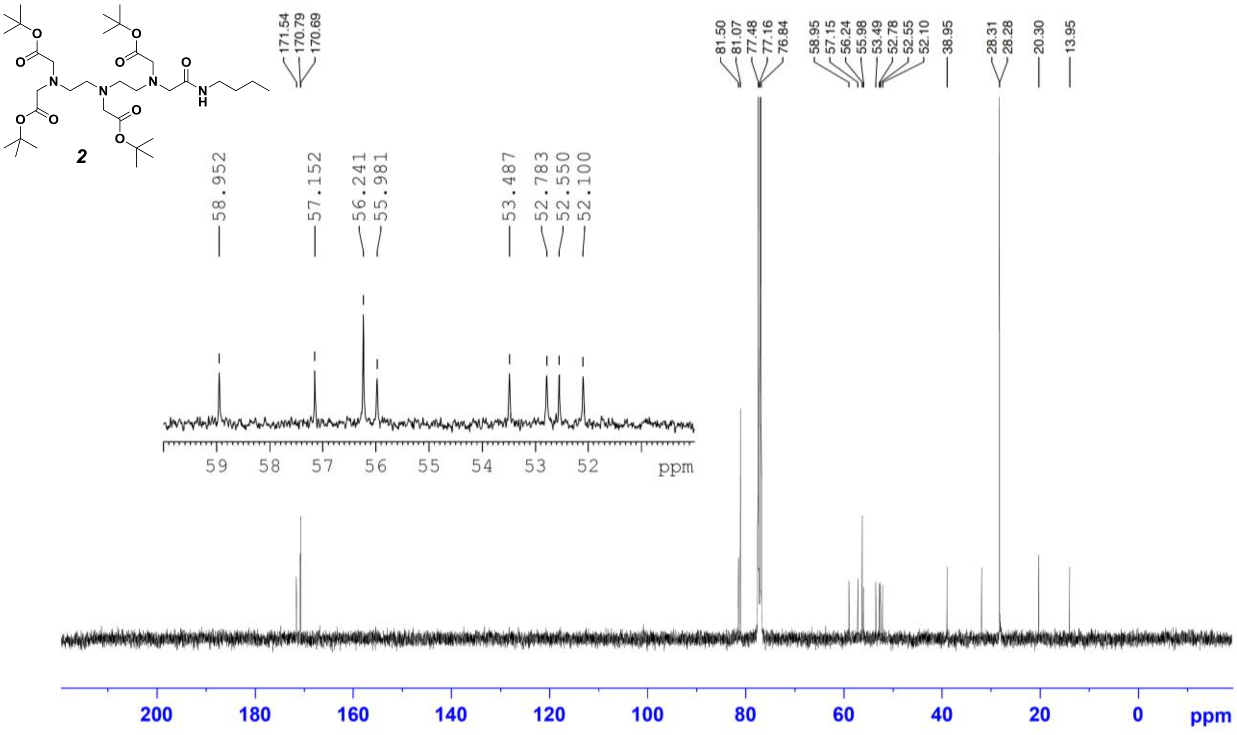

Figure SI-2. ^{13}C NMR spectrum of **2** in $CDCl_3$.

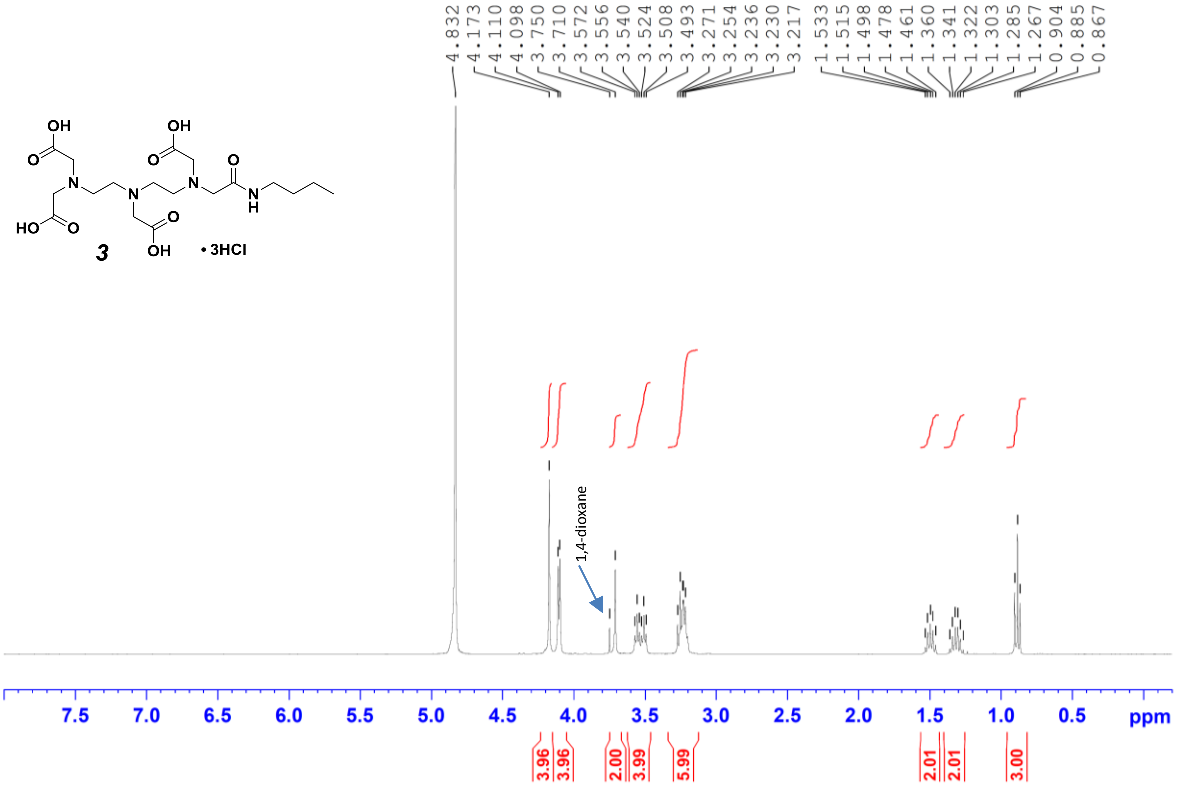

Figure SI-3. ^{1}H NMR spectrum of **3** in D_2O.

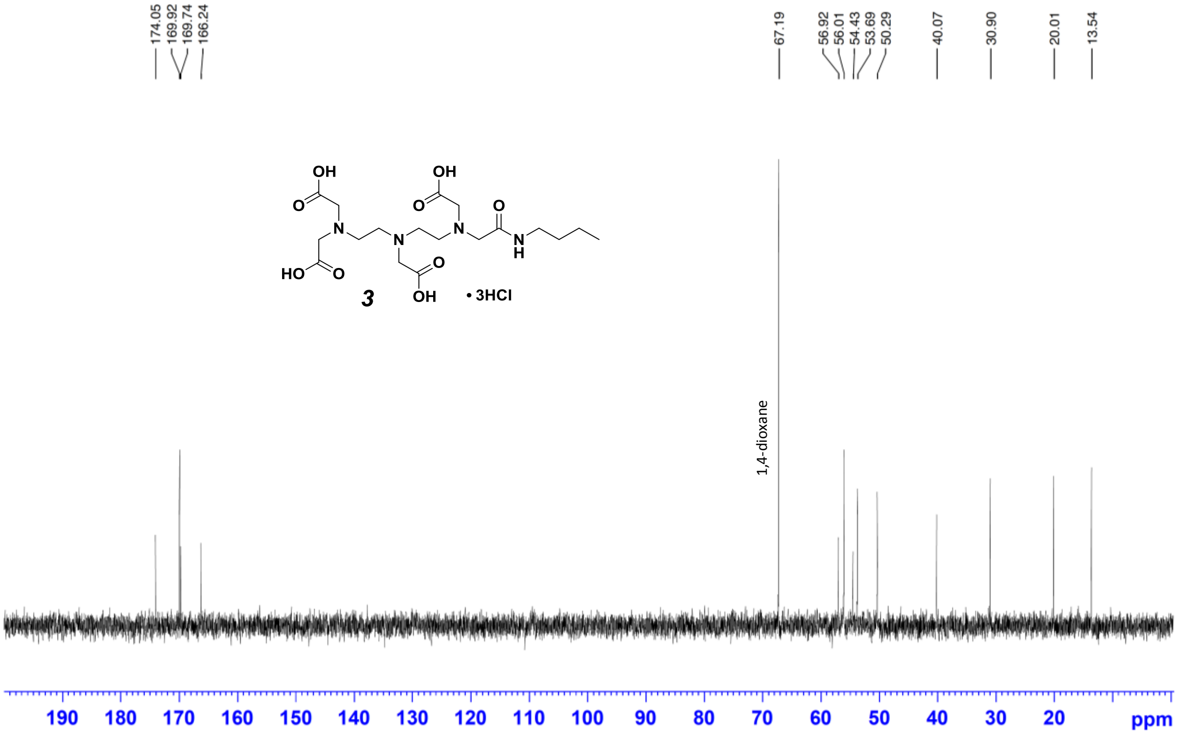

Figure SI-4. ^{13}C NMR spectrum of **3** in D_2O.

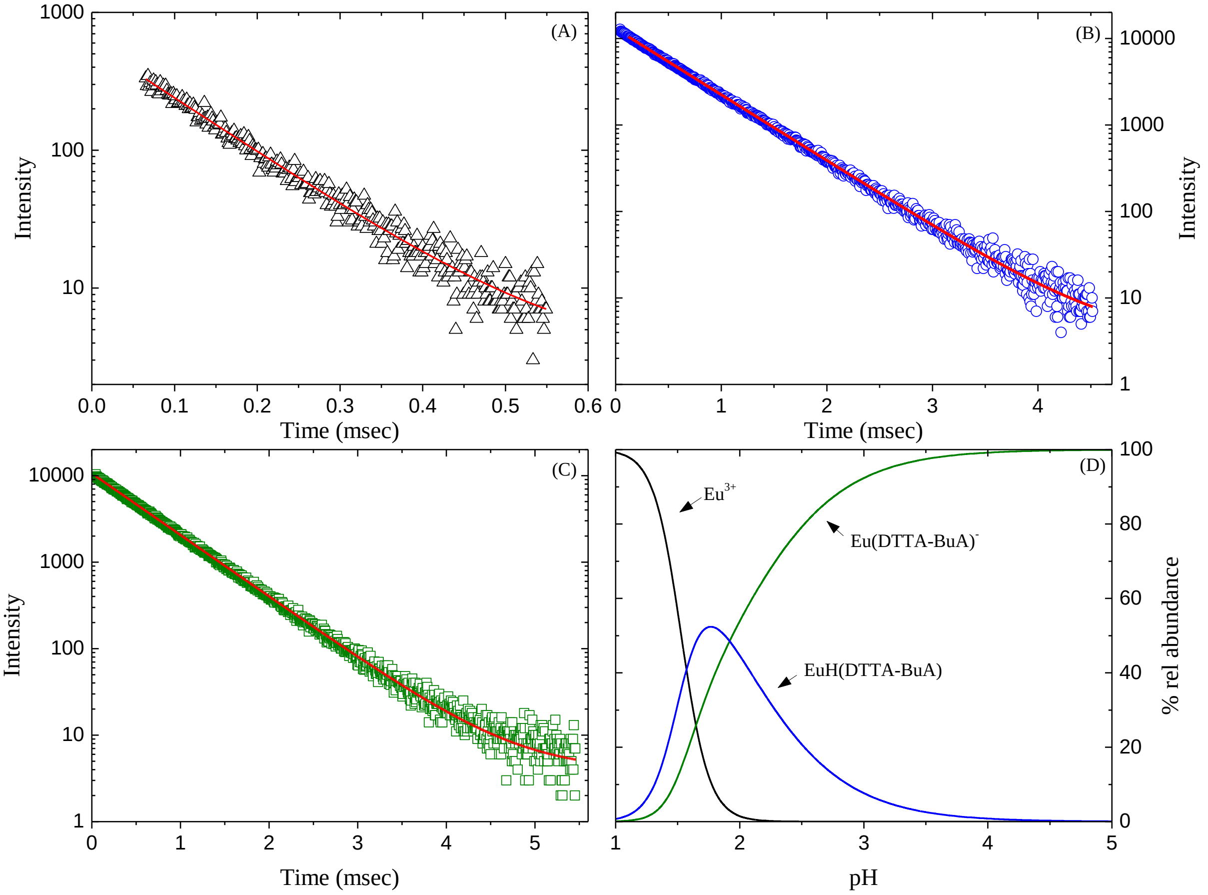

Figure SI-5. Luminescence lifetime studies of Eu(III)/DTTA-BuA solutions at different p[H^+] with T = 25.0 ± 0.01 °C, I = 2.00 M adjusted with (Na/H)ClO_4. **(A)** [$Eu(ClO_4)_3$] = 1.0 mM, [DTTA-BuA] = 10.0 mM and p[H^+] = 0.97 **(B)** [$Eu(ClO_4)_3$] = 1.0 mM, [DTTA-BuA] = 9.6 mM and p[H^+] = 1.77 **(C)** [$Eu(ClO_4)_3$] = 1.0 mM, [DTTA-BuA] = 9.8 mM and p[H^+] = 5.27 **(D)** Speciation plot of 1 mM $Eu(ClO_4)_3$ in the presence of 10 mM DTTA-BuA.

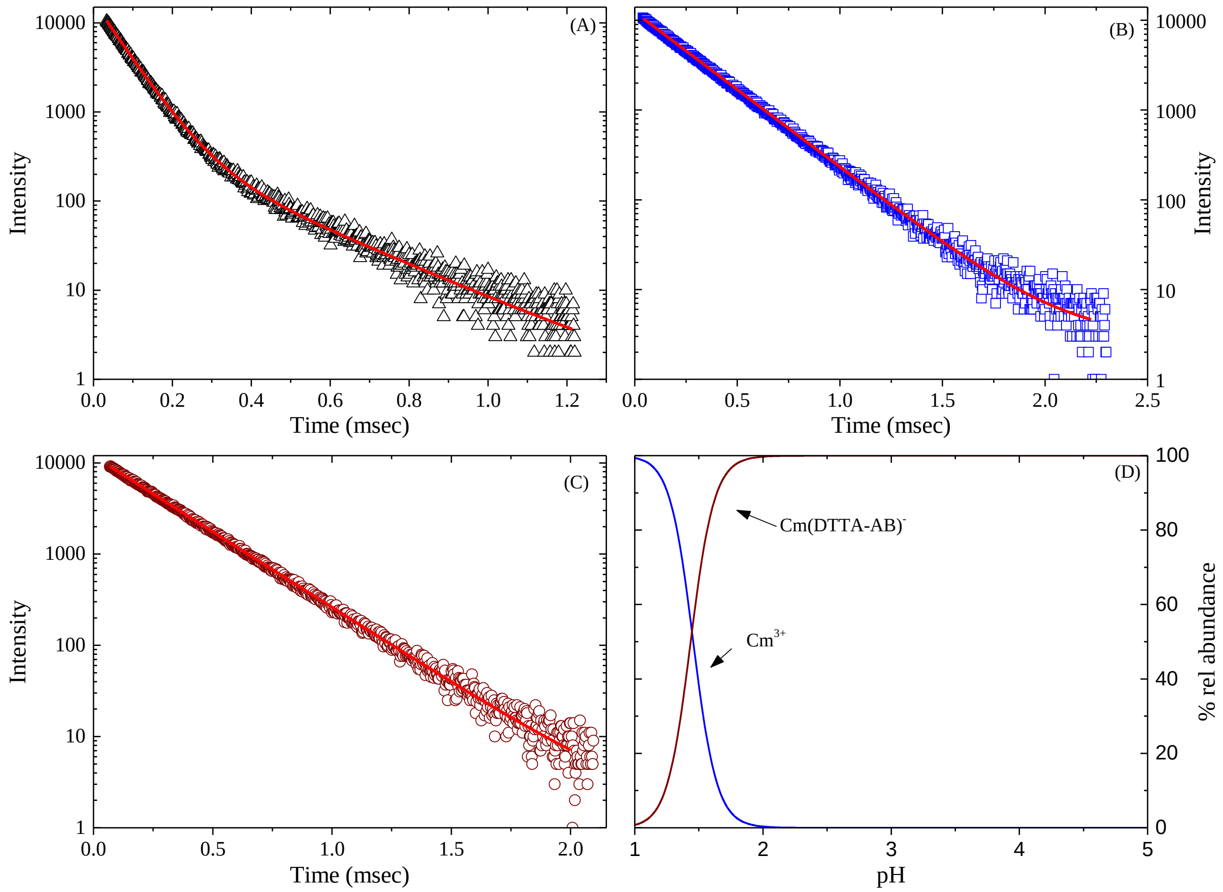

Figure SI-6. Luminescence lifetime studies of ^{248}Cm(III)/DTTA-BuA solutions at different p[H$^+$] with T = 25.0 ± 0.01 °C, I = 2.00 M adjusted with (Na/H)ClO$_4$. **(A)** [Cm(ClO$_4$)$_3$] = 31.0 μM, [DTTA-BuA] = 10.0 mM and p[H$^+$] = 0.97 **(B)** [Cm(ClO$_4$)$_3$] = 31.0 μM, [DTTA-BuA] = 9.6 mM and p[H$^+$] = 1.77 **(C)** [Cm(ClO$_4$)$_3$] = 31.0 μM, [DTTA-BuA] = 9.8 mM and p[H$^+$] = 5.27 **(D)** Speciation plot of 31.0 μM Cm(ClO$_4$)$_3$ in the presence of 10 mM DTTA-BuA.

Table SI-1. M–O and M–N bond distances (Å) in ML$^-$ and MHL complexes (M = Eu/Am) computed at the B3LYP/LC/def2TZVPP level

	EuL$^-$	EuHL	AmL$^-$	AmHL
M-O$_1$	2.377	2.288	2.444	2.354
M-O$_2$	2.367	2.325	2.437	2.393
M-O$_3$	2.380	2.344	2.433	2.408
M-O$_4$/O$_{COOH}$	2.373	2.650	2.444	2.712
M-O$_{water}$	2.641	2.596	2.693	2.652
M-O$_{5amide}$	2.535	2.492	2.605	2.554
M-N$_1$/N$_{CH2COOH}$	2.690	2.843	2.733	2.880
M-N$_2$	2.683	2.666	2.730	2.711
M-N$_{3CH2CONHR}$	2.979	2.863	2.993	2.890

Table SI-2. Natural electron configuration of Eu and Am ions in the studied complexes

Complex	Natural electron configuration
EuL$^-$	[core]6s(0.15)4f(6.10)5d(0.88)6p(0.01)6d(0.05)]
EuHL	[core]6s(0.15)4f(6.10)5d(0.87)6p(0.01)6d(0.05)]
AmL$^-$	[core]7s(0.17)5f(6.15)6d(0.77)7p(0.01)]
AmHL	[core]7s(0.16)5f(6.14)6d(0.76)7p(0.01)]

Table SI-3. Leading donor−acceptor natural bond orbital (NBO) interactions and their second-order stabilization energies *E*$^{(2)}$ (kcal/mol)

Complex [Natural electron configuration of M in the complex]	Donor NBO–acceptor NBO[1] in ML$^-$ and MHL, M = Eu/Am				Total
	$\mathrm{LP_{Ocarboxylate}} \rightarrow \mathrm{n^*_M}$ (four carboxylate oxygens)	$\mathrm{LP_{Oamide}} \rightarrow \mathrm{n^*_M}$ (amide oxygen)	$\mathrm{LP_{Oamine}} \rightarrow \mathrm{n^*_M}$ (three amine nitrogens)	Back-donation to $\sigma^*_{O\text{-}C}$, $\sigma^*_{N\text{-}C}$, and Rydberg orbitals of O and N	
EuL$^-$	566.20	88.24	100.58	4.11	759.13
EuHL	540.43	89.83	97.89	3.79	731.94
AmL$^-$	499.64	75.18	93.20	20.68	688.70
AmHL	471.52	80.93	88.50	18.69	659.64

[1] The unstarred and starred labels correspond to Lewis (donor) and non-Lewis (acceptor) NBOs, respectively. Functional groups of the ligand contributing to the particular interaction are shown in parentheses. LP denotes an occupied lone pair; n*$_M$ denotes vacant Eu/Am orbitals.

The calculated natural orbital occupancies indicate that among metal orbitals, the vacant Am 6d and Eu 5d orbitals are the main contributors to the bond (Table SI-2). The NBO population on Am 6d (0.77 |e|) is considerably less than that on Eu 5d (0.88 |e|). However, charge transfer from the ligand occupied orbitals is higher for Am 5f (0.15 |e|) and 7s (0.17 |e|) than for Eu 4f (0.10 |e|) and 6s (0.15 |e|) orbitals. The populations of Am/Eu 7p/6p and 7d/6d orbitals are negligibly small (Table SI-2). Therefore, these orbitals do not play a significant role in the metal-ligand interactions. Overall, after summation of the f, d, and p orbital occupancies in the considered complexes, the charge transfer from the ligand to the trivalent metal ion is larger for Eu(III) than for Am(III), which is consistent with a smaller ionic radius and higher charge density on Eu(III). A more detailed analysis of the role of individual ligand donor groups in metal-ligand bonding was performed using the second order perturbation theory (SOPT), and the results are summarized in Table SI-3. Figure SI-7 demonstrates the representative forward (ligand to metal) donations, which primarily involve directional sp hybridized (s40%; p60%) oxygen and nitrogen donor lone pairs that overlap favorably with the acceptor Am/Eu orbitals. A detailed SOPT analysis of the donor-acceptor interactions in Table SI-3 shows that AmL^- (27.1 kcal/mol) and EuL^- (26.9 kcal/mol) complexes are almost equaly stabilized by forward donation contributions compared to their protonated analogs. However, this is not the case when comparing back-donation contributions that more strongly stabilize AmL^- *vs.* AmHL (2.0 kcal/mol) than EuL^- *vs.* EuHL (0.3 kcal/mol).

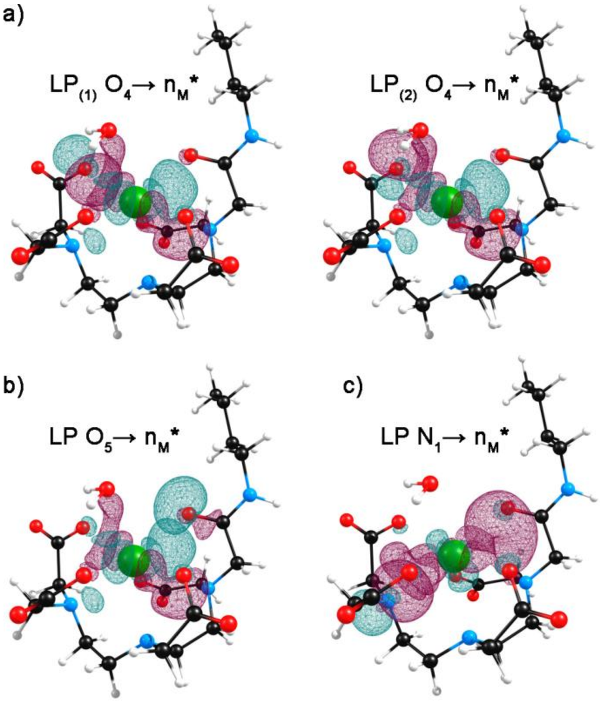

Figure SI-7. The interacting donor – acceptor natural bond orbitals: a) two sp hybridized oxygen lone pairs ($LP_{(1)O4}$ and $LP_{(2)O4}$) – df hybridized vacant metal orbital (n^*_M); b) sp hybridized oxygen lone pair (LP_{O5}) – df hybridized vacant metal orbital (n^*_M); c) sp hybridized nitrogen lone pair (LP_{N1}) – sdf hybridized vacant metal orbital (n^*_M).

References

---

[1] Inam, A.; Van Zyl, R. L.; van Vuuren, N. J.; Chen, C.-T.; Avecilla, F.; Agarwal, S. M.; Azam, A. *RSC Advances*, **2015**, *5*, 48368−48381.